**The EMBO Journal** Vol.16 No.24 pp.7287–7296, 1997

# Perforin is activated by a proteolytic cleavage during biosynthesis which reveals a phospholipid-binding C2 domain

**Ruth Uellner[1], Marketa J.Zvelebil[2], Jean Hopkins[3], Jane Jones[3], Lindsay K.MacDougall[2], B.Paul Morgan[3], Eckhard Podack[4], Michael D.Waterfield[2,5] and Gillian M.Griffiths[1,6,7]**

MRC Laboratory of Molecular Biology, [1]Departments of Biology, [5]Biochemistry and Molecular Biology, University College London, Gower St, London WC1E 6BT, [2]Ludwig Institute for Cancer Research, 91 Riding House St, London W1P 8BT and [3]Department of Medical Biochemistry, University of Wales College of Medicine, Cardiff CF4 4XN, UK and [4]Department of Microbiology and Immunology, University of Miami, Florida, USA

[6]Present address: Sir William Dunn School of Pathology, South Parks Rd, Oxford, OX1 3RE, UK

[7]Corresponding author

**Perforin is a secreted protein synthesized by activated cytotoxic T lymphocytes (CTL) and natural killer (NK) cells. It is a key component of the lytic machinery of these cells, being able to insert into the plasma membrane of targeted cells, forming a pore which leads to their destruction. Here we analyse the synthesis, processing and intracellular transport of perforin in the NK cell line YT. Perforin is synthesized as a 70 kDa inactive precursor which is cleaved at the C-terminus to yield a 60 kDa active form. This proteolytic cleavage occurs in an acidic compartment and can be inhibited by incubation of the cells in ammonium chloride, concanamycin A, leupeptin and E-64. The increased lytic activity of the cleaved form can be demonstrated by killing assays in which cleavage of the pro-piece is inhibited. Epitope mapping reveals that cleavage of the pro-piece occurs at the boundary of a C2 domain, which we show is able to bind phospholipid membranes in a calcium-dependent manner. We propose that removal of the pro-piece, which contains a bulky glycan, allows the C2 domain to interact with phospholipid membranes and initiate perforin pore formation.**
*Keywords*: activation/C2 domain/cytolytic/perforin/phospholipid

## Introduction

Cytotoxic T lymphocytes (CTL) and natural killer (NK) cells play a critical role in the immune system by being able to recognise and directly destroy virally infected and tumorigenic cells. These target cells are destroyed by the release of several cytotoxic proteins which are stored in specialised secretory granules in activated CTL and NK cells, termed lytic granules. Perforin is a key component of the cytolytic machinery: upon secretion it binds and inserts itself into the phospholipid bilayer of the target cell plasma membrane, and polymerises to form a pore of ~16 nm in diameter through the target cell membrane (reviewed in Lowin *et al.*, 1995). This pore induces target cell death in two ways: (i) by osmotic lysis and (ii) by allowing other lytic granule components, most notably granzyme B, to enter the target cell and initiate apoptosis (Darmon *et al.*, 1995, 1996).

Human perforin begins with a signal peptide of 21 amino acids, which is cleaved off in the lumen of the ER. The resulting protein of 534 amino acids contains two potential sites of N-linked glycosylation as predicted from the cDNA sequence (Lichtenheld *et al.*, 1988). The middle of the protein contains an ~300 amino acid stretch of homology to the C9 component of the complement, and is thought to be involved in pore formation, since C9 forms similar pores through lipid bilayers. The C- and N-termini are unique to perforin, and the precise roles of these regions are not known.

Although perforin destroys target cells efficiently, it is not harmful to the cells in which it is synthesized, and several mechanisms are thought to contribute to this. The lytic granules in which the perforin is stored are acidic compartments containing proteoglycans (reviewed in Griffiths and Argon, 1995). The low pH of these organelles is believed to favour the interaction of perforin with the proteoglycans (Masson *et al.*, 1990). The binding of perforin to phospholipid bilayers and the homo polymerization within the membranes are both calcium-dependent processes (Blumenthal *et al.*, 1984; Podack *et al.*, 1985; Masson *et al.*, 1990). It is thought that upon secretion, both pH and calcium concentrations increase, favouring the release of perforin from the proteoglycans and its binding and insertion in the plasma membranes of target cells (Masson *et al.*, 1990). Although this would explain how perforin is kept inactive prior to secretion within the lytic granules, it does not explain how perforin is kept inactive during its biosynthesis when it passes through membrane bound compartments with more neutral pH and high $Ca^{2+}$ concentrations, such as the ER.

The human NK cell line, YT (Yodoi *et al.*, 1985), synthesizes perforin constitutively. Using this cell line, we have studied perforin biosynthesis and the mechanisms which lead to its activation and calcium-dependent binding to phospholipid membranes. We demonstrate that perforin is synthesized as an inactive precursor, and cleaved upon entering an acidic compartment. Only the cleaved form is stored in the granules for secretion. Synthesis of perforin as an inactive precursor protects CTL and NK from perforin-mediated damage during biosynthesis.

## Results

### *Perforin is modified during biosynthesis*

Several forms of perforin were detected using an anti-peptide antibody, 2d4-perf (Baetz *et al.*, 1995), directed

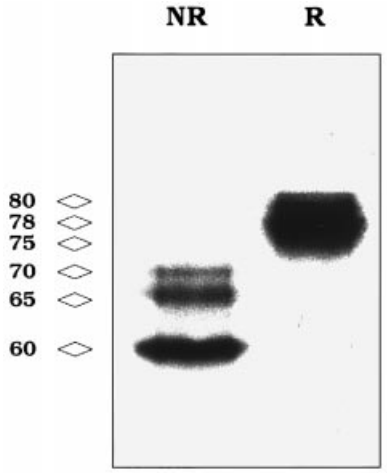


**Fig. 1.** Perforin contains intramolecular disulfide bonds. Cell lysate from the NK cell line YT was run under non-reducing (NR) and reducing (R) conditions, and analysed by Western blotting using the antibody 2d4-perf. Molecular weights are indicated.

against a central region of the protein (Figure 1). Under non-reducing conditions these bands migrate with apparent molecular weights estimated as 60, 65 and 70 kDa, whereas under reducing conditions these bands show apparent molecular weights of approximately 75, 78 and 80 kDa. Non-reducing conditions provide the best separation of the three forms and show that the lowest molecular weight band is the dominant form. The difference in migration on SDS–PAGE under reducing and non-reducing conditions indicates that intramolecular disulfide bridges cause perforin to adopt a more compact form which migrates with an apparently lower molecular weight than the reduced form.

In order to identify the mature form of perforin from the biosynthetic precursors, YT cells were metabolically labelled for 30 min, chased for different lengths of time, immunoprecipitated with the antibody δG9 (which recognises native perforin) and analysed by SDS–PAGE under non-reducing conditions (Figure 2A). After 0 min, chase perforin migrates as a 65 kDa form. After 1 h, >50% matures to a 70 kDa intermediate. Within 5 h, almost all of the perforin migrates as a 60 kDa form, indicating that perforin undergoes cleavage and/or a conformational change which results in an increased mobility on SDS–PAGE.

Endo H treatment of perforin after 0 h chase results in a complete reduction of mobility from 65 kDa to 60 kDa under non-reducing conditions, indicating that the 65 kDa precursor of perforin contains only high-mannose glycans (Figure 2A). The 70 kDa form, which appears after 1 h of chase, is resistant to Endo H digestion, indicating that the N-linked glycans have been further modified to become complex glycans. Some of the 65 kDa precursor is still present after 1 h chase, and this form is reduced to a size of 60 kDa upon glycosidase treatment, as it was at 0 h time point. The mature 60 kDa form of perforin, which appears by 5 h of chase, is resistant to Endo H (Figure 2A), although glycans can be removed by PNGase F treatment, yielding two bands of ~58 kDa and 60 kDa (Figure 2B). These data indicate that both the 70 kDa intermediate and the 60 kDa mature forms of perforin contain only complex glycans.

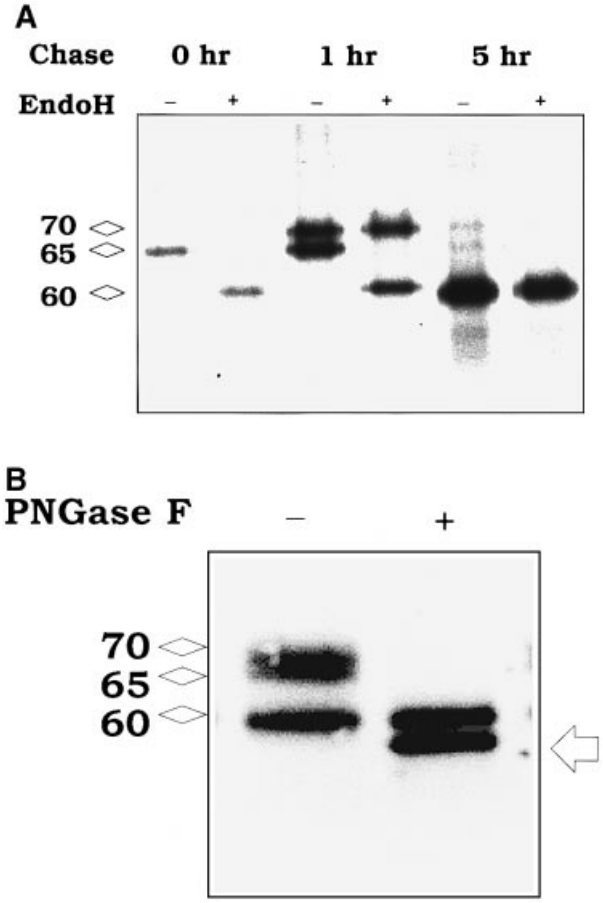


**Fig. 2.** (**A**) Mature perforin contains only complex glycans. YT cells were pulsed and chased for 0, 1 and 5 h, and perforin was immunoprecipitated using the antibody δG9. Samples were treated or untreated with Endo H and analysed by SDS–PAGE under non-reducing conditions. Molecular weights are indicated. (**B**) PNGase F digestion of perforin. Cell lysate was digested with PNGase F and analysed by SDS–PAGE under non-reducing conditions on a 10% gel and detected after Western blot using the antibody 2d4-perf. Molecular weights are indicated. The arrow indicates the de-glycosylated perforin of approximately 58 kDa.

### *Proteolytic cleavage occurs in an acidic compartment*

We asked whether the increase in perforin mobility during its maturation was due to proteolytic cleavage by treating the cells with leupeptin, a reversible inhibitor of serine and cysteine proteases. Figure 3A shows that leupeptin inhibits the processing of the 70 kDa intermediate form to the 60 kDa mature form. After incubation of YT cells with 100 μg/ml leupeptin, there is a decrease in the appearance of the 60 kDa mature form of perforin and an increase in the appearance of the 70 kDa intermediate form, indicating that cleavage to the mature form is inhibited by leupeptin. The degree of inhibition increased with the length of incubation, with ~25% inhibition at 5 h and 50% at 16 h, most probably reflecting increasing uptake of the inhibitor by the cells with time (Seglen, 1983). The cysteine protease inhibitor, E-64, also inhibits the cleavage of perforin to the mature form and results in an ~5-fold increase in the amount of the immature 70 kDa form after a 5 h incubation. In contrast, pepstatin A, an inhibitor of aspartic proteases, does not affect the processing of perforin after 5 h (Figure 3B) or 16 h (data not

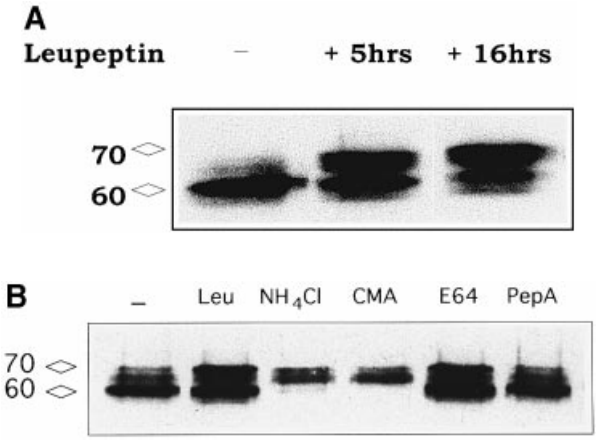


**Fig. 3.** Inhibition of perforin processing. (**A**) YT cells were cultured in the presence or absence (–) of 100 μg/ml leupeptin for 5 h and 16 h, and cell lysates were analysed by SDS–PAGE under reducing conditions and Western blotting using the antibody 2d4-perf. Molecular weights are indicated. (**B**) YT cells were incubated in the presence or absence (–) of inhibitors for 5 h and cell lysates were analysed by SDS–PAGE under reducing conditions and Western blotting using the antibody 2d4-perf. Inhibitors were: leupeptin 20 μg/ml (leu); ammonium chloride 10mM ($NH_4Cl$); concanamycin A 100 ng/ml (CMA); E-64 10 μg/ml; pepstatin A 10 μg/ml (PepA). Molecular weights are indicated.

shown). These results suggest that the processing enzyme is most likely to be a cysteine protease, as the processing is inhibited by leupeptin and E-64.

We next asked whether proteolysis occurs in an acidic compartment. Treating the cells with either 10 mM ammonium chloride, which increases the pH of endosomal compartments, or 100 ng/ml Concanamycin A (CMA), an inhibitor of the proton pump which maintains acidity in endosomes as well as the lytic granules (Kataoka *et al.*, 1994), for 5 h inhibits the cleavage to the 60 kDa cleaved form completely (Figure 3B). These results indicate that perforin maturation occurs by proteolytic cleavage in an acidic compartment.

### *Cleavage occurs at the C-terminus*

In order to establish the site of proteolytic cleavage, we derived several epitope-specific antibodies against perforin (Figure 4A). Rabbit antisera were raised against an N-terminal region, corresponding to amino acids 23–33 of human perforin (P1), and two C-terminal regions corresponding to amino acids 515–518 (P2) and 522–534 (P3). Antiserum P3 recognizes only the uncleaved immature and intermediate forms of perforin, while P2 preferentially recognizes the mature cleaved form (Figure 4B). These results indicate that cleavage occurs at the C-terminus between the epitopes recognized by P2 and P3 antisera. P3 recognizes the epitope which is cleaved, and cannot recognize the mature form of perforin. Most likely, P2 preferentially recognizes the cleaved form, because removal of the C-terminal peptide and glycan now allows binding of this antibody to its epitope. Since P2 and P3 recognize adjacent epitopes, this indicates that cleavage removes only ~20 amino acids. Although this should account for a decrease in size of ~2 kDa, the cleaved region contains one of the sites of N-linked glycosylation, and therefore cleavage will remove the peptide (~2 kDa) and a glycan (~3 kDa), hence the greater

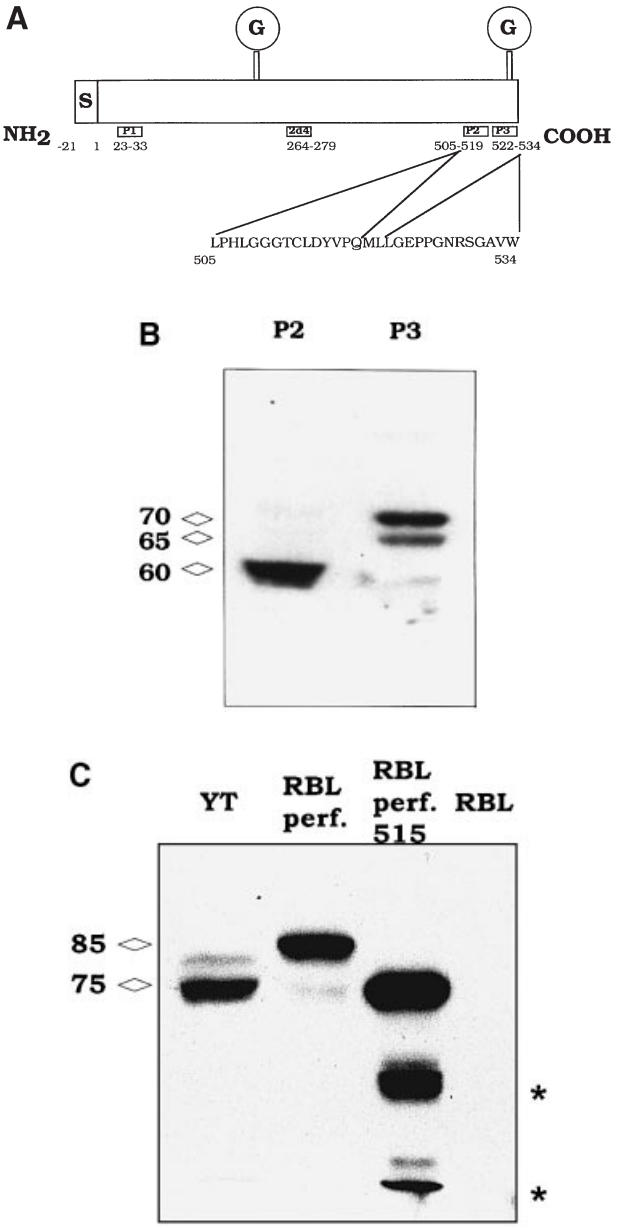


**Fig. 4.** (**A**) Epitope-specific antibodies for perforin. Four epitope-specific antibodies were raised against perforin. The amino acids of human perforin recognized by three rabbit antisera (P1–P3) and one monoclonal antibody (2d4-perf) are shown. The sequences recognized by P2 and P3 are shown. These epitopes are separated by 2 amino acids. Also indicated are the signal sequence and the relative positions of the N-linked glycans. Numbering excludes the signal peptide. (**B**) The epitope recognized by P3 is absent from mature perforin. YT lysate was run under non-reducing conditions and analysed by Western blotting using antibodies P2 and P3. Molecular weights are indicated. (**C**) Perforin lacking the C-terminal 19 amino acids migrates as mature perforin. Lysates from YT, RBL and RBL transfected with wild-type perforin (RBLperf) or a truncation mutant lacking the last 19 amino acids (RBL-perf 515) were analysed by SDS–PAGE under reducing conditions and Western blotting using the antibody 2d4-perf. Molecular weights are indicated and the asterisks mark likely degradation products.

decrease in size of 5 kDa observed under reducing conditions after SDS–PAGE.

To confirm that the C-terminal cleavage of ~20 amino acids would result in the shift in mobility observed, both wild-type perforin and a truncated form of perforin from

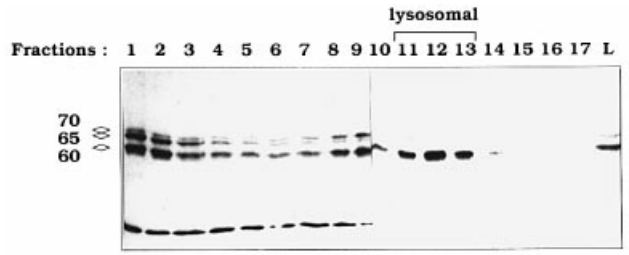


**Fig. 5.** Mature perforin is localised in the lytic granules. YT cells were homogenised and fractionated over a Percoll gradient. 2 ml fractions were analysed by SDS–PAGE under non-reducing conditions and Western blotting using the antibody 2d4-perf. Fraction 1 represents the lightest fraction, fraction 17 the heaviest. Lysosomal enzyme activity was used to detect the lytic granules and was present in fractions 11–13. Whole cell lysate (L) was run as a control. Molecular weights are shown with diamond markings.

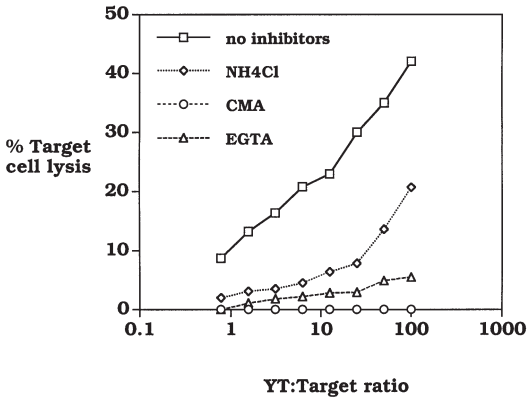


**Fig. 6.** Perforin is activated by proteolytic cleavage. Killing assay using YT cells as the effector cells and the EBV cell line lacking MHC class I, 721.221, as the targets. $^{51}$Cr release from 721.221 cells was measured in a 4 h assay. YT cells were untreated (no inhibitors) or incubated in the presence of inhibitors as shown.

a cDNA lacking the last 19 amino acids were expressed in the mast cell line RBL. The antibody 2d4-perf, which recognizes all three biosynthetic forms, was used to detect perforin in YT and in RBL transfectants after SDS–PAGE under reducing conditions (Figure 4C). In YT, the dominant band is the 75 kDa mature, cleaved form of perforin. Untransfected RBL does not express perforin. In RBL transfected with wild-type perforin, the dominant form is an 85 kDa, uncleaved form equivalent to the 80 kDa form in YT cells. This difference is due to a difference in the size of the glycan modifications (data not shown). The mature, cleaved 75 kDa form is present in RBL, but is much fainter than the equivalent band in YT, suggesting that the cleavage is much less efficient in RBL than YT. In RBL transfected with perforin lacking the last 19 amino acids (RBL perf 515), a band of 75 kDa is observed, demonstrating that removal of the last 19 amino acids and the glycan at asparagine 528 results in a form which co-migrates with the mature form of perforin observed in YT. A smaller band of 50 kDa observed in the truncation mutant is thought to represent a degradation product.

### *Mature perforin is stored in the lytic granules*

The intracellular distribution of the different biosynthetic forms of perforin was examined by subcellular fractionation of YT cells on a Percoll density gradient (Figure 5). Samples from 2 ml fractions were probed with the monoclonal antibody 2d4-perf after Western transfer. Fractions 11–13 were identified as the lytic granule fractions by the presence of the lysosomal enzyme glucosaminidase. Only the mature 60 kDa form of perforin is found in these fractions. All three biosynthetic forms of perforin are present in the lighter fractions (1–10), suggesting that the cleavage may occur before perforin reaches the lytic granule. Fractions 1–3 represent the lightest three fractions at the top of the gradient and may be contaminated by intact cells. The band of 30 kDa is a cross-reacting protein seen by the anti-peptide antibody, 2d4-perf.

### *Ammonium chloride and CMA inhibit perforin-mediated killing by YT*

Since processing to the mature form of perforin is completely inhibited by ammonium chloride and CMA (Figure 3B), we tested the ability of YT cells to kill targets after overnight incubation in 10 mM ammonium chloride or 100 ng/ml CMA. These cells excluded trypan blue, indicating that cell viability was not affected by either treatment. The lytic ability of the cells was assayed by release of $^{51}$Cr from the target cell 721.221. Increasing the number of effector (YT) cells to target cells in a 4 h chromium release assay showed an increase in the percentage of target cells lysed using untreated cells (Figure 6). YT cells treated with ammonium chloride or CMA showed dramatically reduced chromium release from target cells, indicating that perforin-mediated killing is virtually abolished. A similar level of inhibition is seen in cells treated with EGTA, which chelates calcium required for perforin activity.

### *Cleavage exposes a C2-phopholipid binding domain*

Our data demonstrate that activation of perforin occurs after ~20 amino acids, containing a bulky glycan, have been cleaved from the C-terminus of the protein. One possibility is that this peptide and glycan mask a domain of perforin which is required for activity. Several domains of perforin have been identified based on sequence homology to other molecules, but the functions of these domains have never been demonstrated. Interestingly, the C-terminal portion of perforin shows amino acid sequence homology to the C2 domain of protein kinase C. Similar homologies have been found in other proteins including synaptotagmin and phospholipase C delta (PLC-δ) (Brose *et al.*, 1995), in which this domain has been shown to bind phospholipids in a calcium-dependent manner.

Recently the crystal structures of these two C2 domains have been resolved; one for the first domain of synaptotagmin C2A (synC2A) (Sutton *et al.*, 1995), and one for PLC-δ (Essen *et al.*, 1997). Both structures show a β-sandwich formed by eight β-strands, with the calcium binding region formed by the loops at one end of the sandwich. Topologically, the two structures differ, since the β-strands are aligned differently within the barrel (Nalefski and Falke, 1996). We therefore attempted to model the perforin sequence on each of these structures, and found that perforin could be modelled on PLC-δ. Based on this we were able to assign the presumptive lipid binding domain of perforin as being amino acids

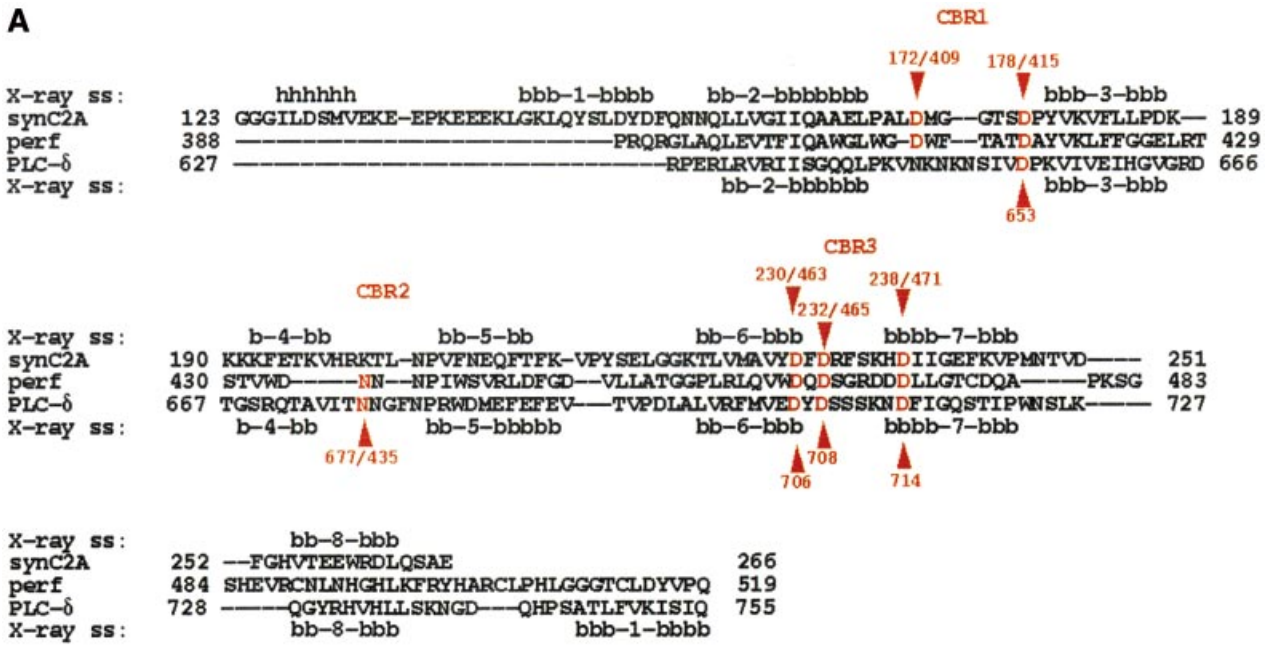


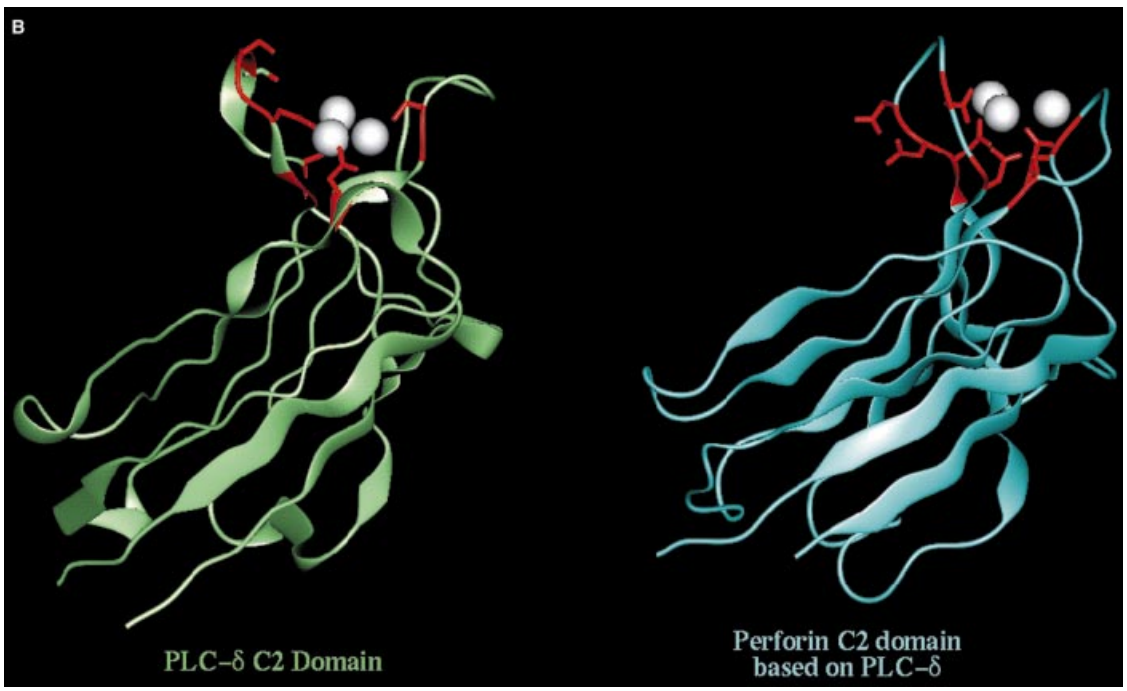


**Fig. 7.** Perforin contains a C2 domain similar to that of PLC delta. (**A**) Sequence alignment of the C2 domains from synaptotagmin C2A (SynC2A), perforin (perf) and phospholipase C delta chain (PLC-δ). The secondary structures determined by the X-ray structures available from synaptotagmin and PLC-δ are shown above and below the alignment respectively (X-ray ss). Amino acid numbering is given for each sequence at the beginning and end of each line. For perforin the numbering does not include the signal sequence. These show helices (h) and β-strands (b). Calcium binding residues are shown in red and these are numbered above the alignment for synC2A, below for PLC-δ and after a / where relevant for perforin. (**B**) Ribbon diagram of C2 domain of PLC-δ and the perforin C2 domain, based on this structure. Aspartic acids in the calcium binding site are shown in red, calcium in white.

388–519 (Figure 7B), with the C2 domain ending at the predicted site of cleavage (Figure 4B).

Figure 7A shows the sequence alignment of these domains with the calcium binding residues shown in red, and Figure 7B shows the ribbon diagram of PLC-δ and the modelled perforin. The calcium binding regions found in PLC-δ and synC2A are conserved in perforin. Two further aspartic acid residues are highlighted in perforin (D469 and D470), which do not align to the aspartic acids that are shown to be involved in binding $Ca^{2+}$ in PLC-δ.

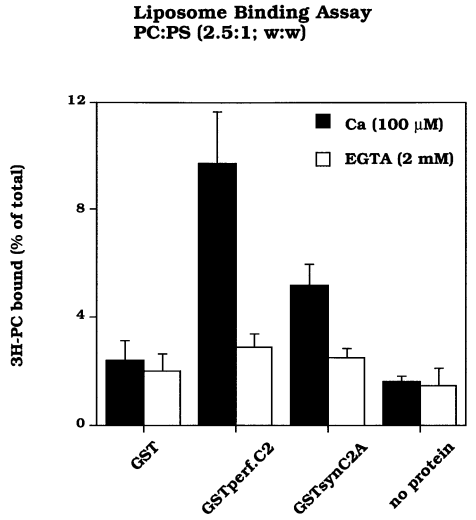


**Fig. 8.** The perforin C2 domain binds phospholipids. GST fusion proteins were used to bind $^3$H labelled PC:PS liposomes. Constructs used were GST alone, GST with the perforin C2 domain, GST with the C2A domain of synaptotagmin or no protein. The percentage of the total counts bound are plotted from an average of three experiments. Mean total c.p.m. = 75 464.

These aspartic acids point away from the pocket (Figure 7A), but may still be involved in increasing the general electrostatic affinity for $Ca^{2+}$ binding.

Although topologically perforin is closer to PLC-δ C2 (with the β-sheets aligning within the β-sandwich in the same order), the amino acid sequence of the first calcium binding regions (CBR1) more closely resembles that of syn C2A. Both perforin and synC2A possess an additional aspartic acid (D409 and D172 respectively) in the first calcium binding region (CBR1) (Figure 7A), while PLC-δ has an asparagine (N645). However, in the second calcium binding region (CBR2), both perforin and PLC-δ contain asparagine residues (N435 and N677 respectively), while synaptotagmin contains a lysine (K200). The X-ray structure of PLC-δ indicates that this asparagine is also involved in calcium binding (Essen *et al.*, 1997). All the other $Ca^{2+}$ binding residues are conserved between all three proteins. Thus it seems that perforin consists of a mixture of synaptotagmin and PLC-δ in CBR 1 and 2, and contains all of the residues required for binding calcium.

In the modelled perforin structure, the calcium-binding aspartic acid residues create a jaw-like structure equivalent to that found in the X-ray structure of PLC-δ. In PLC-δ it has been shown that the binding of calcium causes a structural change, increasing the space between the jaws and allowing binding to a phospholipid head group (Grobler *et al.*, 1996). We wished to test whether a similar mechanism might regulate perforin activity by controlling the binding of the perforin C2 domain to phospholipid membranes. To test whether the perforin C2 domain binds phospholipids in a calcium-dependent fashion, we expressed the C2 domain of perforin as a fusion protein with GST, and assayed the ability of this protein to bind radioactively labelled liposomes. Figure 8 shows that the GST-perforin C2 domain binds phospholipids only in the presence of $Ca^{2+}$. In the absence of $Ca^{2+}$, perforin shows only non-specific levels of binding, comparable with those seen in controls with GST alone or where no protein was added, indicating that the binding of the perforin C2 domain to phospholipids is calcium-dependent. In fact in our studies, the perforin C2 domain always binds phospholipids better than the first C2 domain of synaptotagmin, binding almost twice as well.

## Discussion

Perforin is an important mediator of cell death by the immune system. When secreted from CTL or NK cells in the presence of calcium, it is able to insert into the membrane of the target cell, polymerizing in such a way that it forms a pore through the target cell membrane (reviewed in Lowin *et al.*, 1995). Pore formation causes osmotic lysis of the target, and in addition allows a family of proteases, known as granzymes, to enter and trigger apoptosis. The crucial role played by perforin has been demonstrated in null-mice in which the perforin gene has been deleted, as these mice are unable to clear many viral infections (Kagi *et al.*, 1994; Lowin *et al.*, 1994).

Given perforin's central function in producing a membrane-spanning pore through the target cell membrane, the fact that CTL and NK cells can synthesize and secrete this protein without harming their own membranes is remarkable. One mechanism which has been shown to be important in constraining the action of perforin within CTL and NK cells is its storage within specialized secretory granules, termed lytic granules. These are membrane-bound organelles in which the internal milieu is unfavourable for perforin activity. A proton pump maintains an acidic pH of ~5.5 within these granules (Kataoka *et al.*, 1994, 1996). In addition, these granules are rich in proteoglycans which can form complexes with perforin at acidic pH, and only dissociate when the pH increases during secretion (Masson *et al.*, 1990). It is also likely that $Ca^{2+}$ levels within the granule are very low (although no measurements have been made), since perforin exists as a monomer before secretion, and polymerises in the presence of $Ca^{2+}$. In this way, the cytotoxic cells are able to store active perforin within the granules. However, all secretory proteins pass through the ER during their synthesis, and in this compartment the relatively neutral pH (Mellman *et al.*, 1986) and high calcium concentrations (Montero *et al.*, 1995) would allow active perforin to function, destroying the cell in which it is produced.

Here we demonstrate that perforin is synthesised initially in the ER as a larger precursor protein which is inactive. This precursor is cleaved to the mature, active form and stored in the lytic granules. The ER has been estimated to contain free calcium concentrations in the order of 200 μM (Montero *et al.*, 1995), which is well within the 30–1000 μM range required for maximal perforin activity (Henkart *et al.*, 1984). Along with the neutral pH of this compartment, this environment would allow perforin activity. Synthesis as an inactive precursor prevents membrane damage as perforin passes through the ER and Golgi compartments en route to the lytic granules. Critically, cleavage occurs after perforin has passed through the ER and Golgi, as demonstrated by the fact that inhibitors of endosomal acidification prevent this cleavage. These same findings using inhibitors of endosomal acidification to prevent perforin cleavage also explain earlier observations which showed that ammonium chloride dramatically

reduces cytotoxicity (Savary *et al.*, 1979). Since we are able to demonstrate that the acidification of the lytic granules by either ammonium chloride or CMA prevents cleavage of perforin, and that this cleavage is required for activation, this explains the dramatic reduction in cytotoxicity. These studies suggest that the protease responsible for this cleavage is an acid hydrolase which can be inhibited by leupeptin and E-64, suggesting that a cysteine protease may be responsible for the activation of perforin, consistent with earlier observations that these inhibitors impair perforin activity (Hudig *et al.*, 1984).

What is initially surprising is that the removal of a relatively short piece of the protein (~20 amino acids) can affect the activity of the protein so dramatically. However, two significant changes occur as a result of perforin cleavage. First, removal of the C-terminal amino acids also removes a complex glycan modification of ~3 kDa on N528 within the cleaved piece. It is possible that this bulky glycan contributes to the inhibition of perforin actvity by physically shielding a part of the protein which must be exposed for proper activity. In addition, the cleavage seems to result in a conformational change in perforin, as suggested by the following observation. When run under non-reducing conditions, there is an apparent shift in mobility of ~10 kDa when the mature 70 kDa intermediate is cleaved to the 60 kDa form (Figure 1); however, when the same samples are run under reducing conditions, there is a much smaller shift in mobility from 80 kDa to 75 kDa. This apparent anomaly in size change indicates that the proteolytic cleavage induces perforin to adopt a tighter conformation, which might also be important in the activation of the protein.

One clue as to the mechanism which activates perforin comes from the finding that the predicted cleavage site corresponds to the boundary of a phospholipid-binding C2 domain. The two antisera raised against the C-terminus of perforin predict that the cleavage removes ~20 amino acids of the protein, since the P2 epitope is left intact after cleavage (Figure 4A). Serendipitously, the P2 epitope comprises the end of the C2 domain (Figures 4A and 7A), and demonstrates that cleavage will expose the C2 domain at the C-terminus of the mature perforin. It is therefore possible that the glycan at N528 obscures this domain in the uncleaved perforin, and that exposure of this domain is critical for perforin activity.

Many studies have demonstrated the calcium-dependent nature of perforin activity (Blumenthal *et al.*, 1984); however, the basis of this requirement has not been clear. In this study we demonstrate that the C2 domain identified by sequence homology is a functionally active, calcium-dependent phospholipid binding domain. If the C2 domain is responsible for the initial interaction of perforin with the target cell membrane which leads to pore formation, then the calcium-dependent binding of this domain would determine one calcium requirement for perforin activity. In addition, the binding characteristics of the perforin C2 domain would also determine the binding characteristics of perforin. C2 homology domains have been identified in several different proteins, most of which are involved in the interaction of membranes within the cell (e.g. rab3a and synaptotagmin). Perforin is distinct in being the only extracellular protein in which a C2 domain has been identified, and as such will interact with the outer leaflet

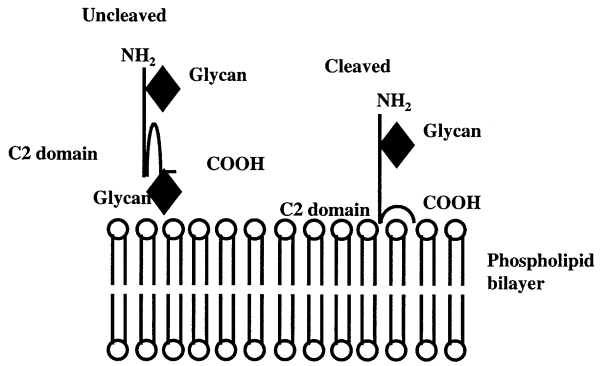


**Fig. 9.** Model of perforin activation. Newly synthesized perforin is unable to bind phospholipid membranes due to the presence of a short C-terminal 'pro-piece' containing a bulky N-linked glycan. Upon cleavage of this pro-piece, the C2 domain of perforin is exposed, able to bind calcium and bind the phospholipid headgroup of the membrane.

of the lipid bilayer. Since the composition of phospholipids within the bilayer is assymetric (Zachowski, 1993), then it is possible that the headgroup specificity of the perforin C2 domain may be distinctive. It has been suggested that phosphorylcholine might act as a receptor for perforin (Tschopp *et al.*, 1989), in which case the C2 domain might also show some specificity for phosphorylcholine. We do not address this question in this study. Our preliminary studies have failed to show headgroup specificity of the perforin C2 domain, and rather seem to support the finding that perforin specificity may be sensitive to headgroup spacing rather than composition (Antia *et al.*, 1992).

Although the binding of perforin to phospholipids is known to be calcium-dependent, the polymerization step is also calcium-dependent (Henkart *et al.*, 1984). Interestingly, calcium-dependent binding to phospholipid membranes is not the only function which has been demonstrated for C2 domains. In the presence of calcium, the second C2 domain of synaptotagmin (synC2B) is able to form oligomers (Sugita *et al.*, 1996). This raises the possibility that the critical polymerization of perforin to form the pore within the phospholipid membrane might also be mediated by the C2 domain in a calcium-dependent manner.

Our findings suggest that the C2 domain of perforin is critical for its activation and function, and we propose a model for perforin biosynthesis and activation, outlined in Figure 9. Newly synthesised perforin contains a short pro-piece of ~20 amino acids containing a modified N-linked glycan. During biosynthesis and passage through the ER and Golgi, the bulky glycan modification obscures the C2 domain such that it is unable to bind phospholipid head groups. However, once perforin is cleaved upon reaching the acidic endosomal compartments, the C2 domain is exposed, calcium is able to bind and the jaws of the C2 domain will open so that phospholipid headgroups can be bound. Our data indicate that the cleavage step which activates perforin is also accompanied by a change to a more compact structure which may also be important for its activity. In support of this model, the C-sequences of perforin show that they are highly conserved in mouse (Lowrey *et al.*, 1989), rat (Ishikawa *et al.*, 1989) and man (Lichtenheld *et al.*, 1988; Shinkai

*et al.*, 1989), and all contain C2 homology domains and glycosylation sites.

Interestingly, we find that the truncation mutant of the C-terminus (perf-515, Figure 4C) is not transported to the secretory granules as wild-type perforin is (Griffiths, 1997), but is retained in the ER as revealed by immunofluoresence (data not shown). Furthermore this truncated perforin is susceptible to degradation (Figure 4C), suggesting that without the C-terminal piece, perforin is misfolded and does not escape the quality control mechanisms of the ER. A series of five other truncation mutants terminating at amino acids 520, 521, 522, 524 and 529, as well as two glycosylation mutants at N528 and S530, are all similarly retained in the ER and readily degraded (R.Uellner and G.M.Griffiths, unpublished). These observations explain why RBL transfected with the truncated form are not killed, since the misfolded protein is highly unlikely to be active. In addition, these findings suggest that the C-terminal piece is required for perforin to be correctly folded and leave the ER. This requirement will prevent active perforin from being expressed in the ER.

These studies suggest that the binding of perforin to membranes leading to pore formation may be critically determined by the binding properties of the C2 domain. This may provide the key to understanding why the membranes of perforin-producing cells are able to resist perforin attack when target cells are destroyed.

## Materials and methods

### *Reagents and antibodies*

Protease inhibitors and endoglycosidase H were from Boehringer Mannheim, $^{51}$Chromium (1 mCi/ml) and the ECL Western Blotting detection Reagent from Amersham Corp., ammonium chloride and NP-40 (Igepal CA 630) from Sigma, CMA was ordered from Calbiochem, Protein G-Sepharose 4 Fast Flow was from Pharmacia Biotech. AB, and the $^{35}$S Protein labelling mix from NEN DuPont.

The monoclonal antibody to human perforin (perf-2d4), derived against the synthetic peptide (KHKMTASFHQTYRERH) corresponding to amino acids 264–279 of the human perforin sequence, has been described elsewhere (Baetz *et al.*, 1995). The mouse anti-perforin antibody δG9 belongs to the IgG2b subclass, and was generated as described against lytic granules isolated from YT (Hameed *et al.*, 1992). The rabbit antisera against the N- and C-terminal regions of perforin (P1, P2 and P3) were generated against MAP-peptides at the Basel Institute for Immunology. These corresponded to the sequences P1: AGEGVDVTSLR (amino acids 23–33); P2: LPHLGGGTCLDYVP (amino acids 505–519); and P3: LGEPPGNRSGAVW (amino acids 522–534). Goat anti-mouse kappa light chain and goat anti-rabbit Ig coupled to horseradish peroxidase antibodies were purchased from Southern Biotechnology, Birmingham, AL, USA.

### *Cells*

The human NK cell line, YT (Yodoi *et al.*, 1985) and the class I deficient EBV transformed B cell line, 721.221, were maintained in RPMI, 10% FCS. The rat basophilic leukemia, RBL, a rat mast cell tumor line, was grown in IMDM, 10% FCS.

### *SDS–PAGE and Western blot*

Cells were washed once in PBS, resuspended at $10^7$ cells/ml in lysis buffer (50 mM TrisCl, pH 8; 150 mM NaCl; 1 mM $MgCl_2$; 2% NP-40) with protease inhibitors and incubated on ice for 30 min. Lysates were spun for 15 min at 13 800 *g* (13 000 r.p.m. using Heraeus Sepatech, rotor 3765) at 4°C and aliquots of 10 µl were resolved by SDS–PAGE on gels of 7.5% acrylamide in a Bio-Rad Mini-PROTEAN II Electrophoresis Cell.

Proteins were transferred to nitrocellulose (Hybond-C extra, Amersham), using a MiniTrans-Blot Apparatus (Bio-Rad) in 25 mM Tris, 192 mM glycine, 20% methanol, pH 8.3. Filters were then blocked for 1 h at room temperature in 5% non-fat dried milk in PBS, 0.1% Tween 20 and then incubated with the primary antibody diluted in PBS, 0.1% Tween 20 for 2–16 h. The filters were washed three times in PBS, 0.1% Tween 20 for 10 min each, incubated with a horseradish peroxidase-labeled anti-Ig secondary antibody, washed three times, developed for 1 min in ECL Western blotting detection Reagent (Amersham) and exposed for times varying between 30 s and 10 min to Biomax MR-1 film (Kodak). As molecular weight standards, 5 µl of the Rainbow$^{TM}$ Marker high range (1 mg/ml of each protein; Amersham), were loaded on a minigel.

### *Deglycosylation of glycoproteins*

For endoglycosidase H (EndoH) treatment, samples were incubated with EndoH at 37°C for 12–16 h in 9 mM $CaCl_2$ and 50 mM sodium acetate, pH 5.5 in the presence of 1 mM Pefabloc (Boehringer Mannheim, Germany). Samples in 0.1% Triton X-100 treated with Peptide-N-glycosidase F (PNGase F) (Boehringer Mannheim) were first denatured in 0.5% SDS at 95°C for 5 min, the SDS was quenched by addition of 2-fold excess of nonionic detergent, and the enzyme added for 12–16 h at 37°C.

### *Metabolic labelling and immunoprecipitation*

For pulse–chase experiments, cells were preincubated for 20 min in methionine/cysteine-free medium supplemented with 10% dialysed fetal calf serum and labelled at 1–2×$10^7$ cell/ml for 30–45 min with 200 µCi/ml L-[$^{35}$S]-Methionine Labelling Mix (NEN DuPont), specific activity >1000 Ci/mmol. Pulse-labelled cells were then chased for 1–5 h in complete RPMI, 10% FCS. Any inhibitors were added after the labelling. Between 5×$10^6$ and 1×$10^7$ cell were lysed in 1 ml lysis buffer (see SDS–PAGE), pre-cleared by incubation with 10 µl normal mouse serum and then Protein G-Sepharose for 30 min rotating at 4°C. Perforin was precipitated with 2 µl of δG9 overnight and then 30 min with Protein G-Sepharose at 4°C. After washing three times in cold PBS, 0.1% NP-40, the precipitates were eluted in 20 mM Tris, pH 7, 0.5% SDS for 5 min at 95°C. Eluates were resolved by SDS–PAGE. Each lane represents 1.25–2.5×$10^6$ cells. Gels were fixed, processed with Amplify (Amersham) and dried before exposure to Biomax MR-1 films.

### *Cell cytotoxicity*

YT natural killer cells were incubated with either CMA (100 ng/ml), $NH_4Cl$ (10 mM) or in the absence of inhibitors for 16 h before the killing assay. Cell viability was confirmed using trypan blue exclusion. Cells were then washed twice and resuspended at 5×$10^6$/ml in RPMI, 10% FCS in the presence or absence of the same inhibitors before plating in serial dilutions of 1:2 into a 96-well plate to give the effector:target ratios shown. Pelleted 721.221 target cells were labelled with 100 µCi $^{51}$Cr in 100 µl for 90 min, washed in PBS containing 1% FCS at 37°C three times to get rid of unincorporated radioactivity and resuspended at 5×$10^4$ cells/ml in RPMI, 10% FCS. One hundred µl/well were added to the killer cells, plates spun gently at 235 *g* (1000 r.p.m. using Heraeus Varifuge, rotor 8079) for 2 min and incubated at 37°C for 5 h. EGTA was added to one set of the targets to 4 mM (= 2×) before plating out. All samples were plated in triplicate. Before harvesting, the plates were spun again and 100 µl of supernatant from each sample was counted in a gamma counter. The percentage of specific target cell lysis was calculated as equal to (experimental release – spontaneous release) / (total release – spontaneous release). For the spontaneous release, target cells were incubated in RPMI ± inhibitors without any killer cells, whereas the total release was measured by lysing targets with 5% NP-40.

### *Cell fractionation and glucosaminidase assay*

Twenty million YT cells were washed three times in PBS and once in 50 mM HEPES, pH 7.2, 90 mM KCl. Cells were resuspended in a minimum of 6 ml of HEPES/KCl or 5-fold the volume of the pellet, whichever was greater. Cells were disrupted at 4°C by passing them through the ball bearing cell homogeniser 20 times using a ball bearing of 8.006 mm diameter. Lysis was verified under the microscope when the lysis buffer appeared grainy owing to the presence of organelles. Nuclear material was spun out at 1040 *g* (2000 r.p.m. using Heraeus Varifuge, rotor 8079) for 4 min at 4°C. The pellet was washed once in 4 ml HEPES/KCl buffer and added to the soluble fraction to make a final volume of 10 ml. Using a stock of 90 ml Percoll (Pharmacia, Uppsala, Sweden) with 10 ml 500 mM HEPES, pH 7.2, 900 mM KCl, a Percoll step gradient was formed by underlaying 15.9 ml 39% Percoll with 12.1 ml 90% Percoll. All dilutions of Percoll were made in 50 mM Hepes, pH 7.2, 90 mM KCl. The soluble cell lysate was then overlayed onto this gradient and centrifuged at 40 000 *g* (15 000 r.p.m. using a TST 28.38 Kontron rotor) for 30 min at 4°C. The top 10 ml of soluble

lysate which did not enter the gradient were removed, discarded and 1 ml fractions were collected from the top of the gradient. Samples of each fraction were assayed for glucosaminidase activity: 20 µl samples of each fraction were diluted in 200 mM citric acid, pH 4.5, 0.2% Triton X-100, and incubated in the presence of 8 mM p-Nitrophenyl *N*-Acetyl-β-D-glucosaminide (Sigma) for 30 min at 37°C. The reaction was stopped by the addition of 1 ml 67 mM NaCl, 83 mM $Na_2CO_3$, 33 mM glycine pH 10.5, and the absorbance read at 405 nm. Background levels were >0.07 and only fractions 11–13 showed higher values of 0.083, 0.157 and 0.124 respectively.

### *Transfection into RBL*

Perforin 1–515 was generated by PCR and cloned into pSRαSD7. Eighteen µg DNA were linearized and co-transfected with 2 µg pfneo containing the neomycin resistance gene into $10^7$ RBL by electroporation at 250 V and 500 µF. Cells were grown in medium containing 5% FCS for 24 h before adding geneticin (Gibco) at 1 mg/ml to select stable transfectants. Perforin expression was screened by staining with 2d4-perf.

### *Construction of expression vectors and expression and purification of recombinant proteins*

For the construction of pGEX perf.C2 which encodes the C2 domain of perforin fused to GST, the DNA from human perforin (nucleotides 1225–1632) was amplified by PCR with oligonucleotides 13 005 (CGC GGA TCC CCT CGG CAG AGG GGC CTG) and 13 006 (CGG AAT TCC CCC CAG AAG CAT TTG GGG). The resulting 0.52 kb PCR fragment was subcloned into the *Bam*HI and *Eco*RI sites of the bacterial expression vector pGEX-2T (Pharmacia) and confirmed by sequencing. Recombinant proteins were produced in *Escherichia coli* Top10F′ bacteria. Typically, bacteria were grown at 30°C to an $OD_{600}$ of 0.5–0.6 before IPTG was added to 1 mM and cultures incubated for a further 2 h. Pelleted cells were resuspended in 20 ml PBS, 1% (w/v) Triton X-100 with protease inhibitors (Complete™, Boehringer), lysed by sonication and centrifuged at 4000 *g*. The supernatant was incubated with 1.6 ml of 50% glutathione–Sepharose beads for 45 min at room temperature with tumbling. GST fusion proteins bound to beads were recovered by centrifugation at 500 *g*, washed several times in PBS-T and PBS and stored as a 50% slurry in 50% Glycerol:PBS plus inhibitors. The protein concentration was determined using the BCA protein assay kit (Pierce Chemical Co.) with the protein still bound to beads. Protein purity and integrity were verified after purification by SDS–PAGE.

### *Liposome preparation and binding assay*

This assay was carried out as described (Schiavo *et al.*, 1996). Six hundred µg phospholipids dissolved in chloroform were mixed in a polypropylene tube and dried under a gentle flow of nitrogen. Liposomes were made from L-α-Phosphatidylcholine (PC) mixed with L-α-Phosphtidyl-L-Serine (PS) (2.5:1; w:w) (Sigma). 3.5 µCi of L-3-Phosphatidyl[N-methyl-$^3$H]choline,1,2,-dipalmitoyl (80 Ci/mmol, Amersham) were added as a tracer. Dried phospholipids were resuspended in 2.5 ml buffer A (20 mM HEPES–KOH (pH 7.6), 100 mM KCl, 0.2 mM DTT) by pipetting up and down. Liposomes were prepared by sonication followed by liposome purification over a Sephadex G-25 M column (PD-10, Pharmacia). 1 ml fractions were collected and an aliquot of each fraction counted by liquid scintillation counting. Usually fractions 4 and 5 contained one-third of the total counts and liposomes of these fractions (~200 µg/ml; 1.16 µCi/ml) were used for the binding assay. Liposomes were centrifuged for 2 min at 13 800 *g* (13 000 r.p.m. using Heraeus Sepatech, rotor 3765) to remove large aggregates and either $CaCl_2$ (100 µM) or EGTA (2 mM) was added to the supernatant. For the binding assay, 15 µg of purified GST fusion proteins containing either the C2 domain of perforin (aa 409–544) or the first C2 domain of rat synaptotagmin I (aa 140–267) (Davletov and Sudhof, 1993; Sutton *et al.*, 1995) (referred to as synC2A) bound to glutathione–Sepharose beads were used. Glutathione–Sepharose beads with no protein bound were added where necessary to obtain the same volume of beads (28 µl of packed beads) in each tube. Beads were prewashed twice in buffer A containing either 100 µM $CaCl_2$ or 2 mM EGTA, resuspended in 140 µl of the same buffer and 100 µl of the $^3$H-labelled liposomes were added. The mixture was incubated at room temperature for 45 min with vigorous shaking and then washed four times with 500 µl incubation buffer. Liposomes bound to beads were solubilized with 0.3 ml of 10% SDS and radioactivity associated with the pellet was determined by liquid scintillation counting. Data shown are the average of three independent experiments ± SD.

### *Alignment of modelling*

Initial alignment of the perforin C2 domain with the structure of the synaptotagmin C2A domain (Sutton *et al.*, 1995) failed to align the first strand. It was not until the structure of phospholipase Cδ (PLC-δ) and the alternative C2 domain topology became available that it became obvious that perforin followed the type II topology used by PLC-δ, and that strand 2 was actually strand 8 (Figure 7B). The initial alignment was obtained using Multalign (GJB), and then modified manually for optimal results taking into account SS information and the calcium binding residues. The model of the perforin C2 domain used the structure of PLC-δ (Essen *et al.*, 1997) as a template. The manually adjusted alignment was used within Quanta™ to transfer eqvuivalent co-ordinates. To build insertions/deletions a high resolution (<2.01Å) fragment database was searched for segments with the appropriate length for close sequence similarity and good fit on the perforin loop ends. These regions were minimized locally before the entire modelled structure was subjected to SD minimization, until the energy fluctuation levelled out.

## Acknowledgements

G.M.G. and R.U. would like to thank Jim Kaufman, Lesley Page, Karin Romisch and G.P.Schiavo for helpful discussions and comments on the manuscript. Co-ordinates for the structure of the C2 domain of PLC-δ were kindly provided by R.Williams. This work was initiated while G.M.G. was at the Basel Institute for Immunology, which was founded by and is supported by F.Hoffman-LaRoche. Most of the work was carried out at UCL and was supported by a Wellcome Trust Senior Fellowship to G.M.G. (# 040825). B.P.M. is also a Wellcome Trust Senior Fellow, J.H. a Wellcome Prize Student and J.J. was supported by the Arthritis Research Council.

## References

Antia,R., Schlegel,R.A. and Williamson,P. (1992) Binding of perforin to membranes is sensitive to lipid spacing and not headgroups. *Immunol. Letts.*, **32**, 153–158.

Baetz,K., Isaaz,S. and Griffiths,G.M. (1995) Loss of cytotoxic T lymphocyte function in Chediak-Higashi syndrome arises from a secretory defect that prevents lytic granule exocytosis. *J. Immunol.*, **154**, 6122–6131.

Blumenthal,R., Millard,P.J., Henkart,M.P., Reynolds,C.W. and Henkart,P.A. (1984) Liposomes as targets for granule cytolysin from cytotoxic large granular lymphocyte tumors. *Proc. Natl Acad. Sci. USA*, **81**, 5551–5555.

Brose,N., Hofmann,K., Hata,Y. and Sudhof,T.C. (1995) Mammalian homologues of *Caenorhabditis elegans* unc-13 gene define novel family of C2-domain proteins. *J. Biol. Chem.*, **270**, 25273–25280.

Darmon,A.J., Nicholson,D.W. and Bleackley,R.C. (1995) Activation of the apoptotic protease CPP32 by cytotoxic T-cell-derived granzyme B. *Nature*, **377**, 446–448.

Darmon,A.J., Ley,T.J., Nicholson,D.W. and Bleackley,R.C. (1996) Cleavage of CPP32 by granzyme B represents a critical role for granzyme B in the induction of target cell DNA fragmentation. *J. Biol. Chem.*, **271**, 21709–21712.

Davletov,B.A. and Sudhof,T.C. (1993) A single C2 domain from synaptotagmin I is sufficient for high affinity $Ca^{2+}$/phospholipid binding. *J. Biol. Chem.*, **268**, 26386–26390.

Essen,L.O., Perisic,O., Lynch,D.E., Katan,M. and Williams,R.L. (1997) A ternary metal binding site in the C2 domain of phosphoinositide-specific phospholipase C-delta 1. *Biochemistry*, **36**, 2753–2762.

Griffiths,G.M. (1997) Protein sorting and secretion during CTL killing. *Semin. Immunol.*, **9**, 109–115.

Griffiths,G.M. and Argon,Y. (1995) Structure and biogenesis of lytic granules. *Curr. Top. Microbiol. Immunol.*, **198**, 39–58.

Grobler,J.A., Essen,L.O., Williams,R.L. and Hurley,J.H. (1996) C2 domain conformational changes in phospholipase C-delta 1. *Nat. Struct. Biol.*, **3**, 788–795.

Hameed,A., Olsen,K.J., Cheng,L., Fox,W.M.D., Hruban,R.H. and Podack,E.R. (1992) Immunohistochemical identification of cytotoxic lymphocytes using human perforin monoclonal antibody. *Am. J. Pathol.*, **140**, 1025–1030.

Henkart,P.A., Millard,P.J., Reynolds,C.W. and Henkart,M.P. (1984) Cytolytic activity of purified cytoplasmic granules from cytotoxic rat large granular lymphocyte tumors. *J. Exp. Med.*, **160**, 75–93.

Hudig,D., Redelman,D. and Minning,L.L. (1984) The requirement for proteinase activity for human lymphocyte-mediated natural cytotoxicty (NK): evidence that the proteinase is serine dependent and has aromatic amino acid specificity of cleavage. *J. Immunol.*, **133**, 2647–2654.

Ishikawa,H. *et al.* (1989) Molecular cloning of rat cytolysin. *J. Immunol.*, **143**, 3069–3073.

Kägi,D., Vignaux,P., Lederman,B., Burki,K., Depraetere,V., Nagata,S., Hengartner,H. and Golstein,P. (1994) Fas and perforin pathways as major mechanisms of T-cell mediated cytotoxicity. *Science*, **265**, 528–530.

Kataoka,T., Takaku,K., Magae,J., Shinohara,N., Takayama,H., Kondo,S. and Nagai,K. (1994) Acidification is essential for maintaining the structure and function of lytic granules of CTL. Effect of concanamycin A, an inhibitor of vacuolar type H(+)-ATPase, on CTL-mediated cytotoxicity. *J. Immunol.*, **153**, 3938–3947.

Kataoka,T., Shinohara,N., Takayama,H., Takaku,K., Kondo,S., Yonehara,S. and Nagai,K. (1996) Concanamycin A, a powerful tool for characterization and estimation of contribution of perforin- and Fas-based lytic pathways in cell-mediated cytotoxicity. *J. Immunol.*, **156**, 3678–86.

Lichtenheld,M.G., Olsen,K.J., Lu,P., Lowrey,D.M., Hameed,A., Hengartner,H. and Podack,E.R. (1988) Structure and function of human perforin. *Nature*, **335**, 448–451.

Lowin,B., Hahne,M., Mattman,C. and Tschopp,J. (1994) Cytolytic T-cell cytotoxicity is mediated through perforin and Fas lytic pathways. *Nature*, **370**, 650–652.

Lowin,B., Peitsch,M.C. and Tschopp,J. (1995) Perforin and granzymes: crucial effector molecules in cytolytic T lymphocyte and natural killer cell-mediated cytotoxicity. *Curr. Top. Microbiol. Immunol.*, **198**, 1–24.

Lowrey,D.M., Aebischer,T., Olsen,K.J., Lichtenheld,M.G., Rupp,F., Hengartner,H. and Podack,E.R. (1989) Cloning and analysis and expression of murine perforin 1 cDNA, a component of cytolytic T cell granules with homology to complement component C9. *Proc. Natl Acad. Sci. USA*, **86**, 247–250.

Masson,D., Peters,P.J., Geuze,H.J., Borst,J. and Tschopp,J. (1990) Interaction of chondroitin sulfate with perforin and granzymes of cytolytic T-cells is dependent on pH. *Biochemistry*, **29**, 11229–11235.

Mellman,I., Fuchs,R. and Helenius,A. (1986) Acidification of the endocytic and exocytic pathways. *Annu. Rev. Biochem.*, **55**, 663–700.

Montero,M., Brini,M., Marsault,R., Alvarez,J., Sitia,R., Pozzan,T. and Rizzuto,R. (1995) Monitoring dynamic changes in free $Ca^{2+}$ concentration in the endoplasmic reticulum of intact cells. *EMBO J.*, **14**, 5467–5475.

Nalefski,E.A. and Falke,J.J. (1996) The C2 domain calcium-binding motif: structural and functional diversity. *Protein Sci.*, **5**, 2375–2390.

Podack,E.R., Young,J.D. and Cohn,Z.A. (1985) Isolation and biochemical and functional characterization of perforin 1 from cytolytic T-cell granules. *Proc. Natl Acad. Sci. USA*, **82**, 8629–8633.

Savary,C.A., Phillips,J.H. and Lotzova,E. (1979) Inhibition of murine natural killer cell-mediated cytotoxicity by pretreatment with ammonium chloride. *J. Immunol. Methods*, **25**, 189–192.

Schiavo,G., Gu,Q.M., Prestwich,G.D., Sollner,T.H. and Rothman,J.E. (1996) Calcium-dependent switching of the specificity of phosphoinositide binding to synaptotagmin. *Proc. Natl Acad. Sci. USA*, **93**, 13327–13332.

Seglen,P.O. (1983) Inhibitors of lysosomal function. *Methods Enzymol.*, **96**, 737–765.

Shinkai,Y., Yoshida,M.C., Maeda,K., Kobata,T., Marayuma,K., Yodoi,J., Yagita,H. and Okumura,K. (1989) Molecular cloning and chromosomal assignment of a human perforin gene. *Immunogenetics*, **30**, 452–457.

Sugita,S., Hata,Y. and Südhof,T.C. (1996) Distinct $Ca^{++}$-dependent properties of the first and second domains of synaptotagmin I. *J. Biol. Chem.*, **271**, 1262–1265.

Sutton,R.B., Davletov,B.A., Berghuis,A.M., Sudhof,T.C. and Sprang,S.R. (1995) Structure of the first C2 domain of synaptotagmin I: a novel $Ca^{2+}$/phospholipid-binding fold. *Cell*, **80**, 929–938.

Tschopp,J., Schafer,S., Masson,D., Peitsch,M.C. and Heusser,C. (1989) Phosphorylcholine acts as a $Ca^{2+}$-dependent receptor molecule for lymphocyte perforin. *Nature*, **337**, 272–274.

Yodoi,J. *et al.* (1985) TCGF (IL 2)-receptor inducing factor(s). I. Regulation of IL 2 receptor on a natural killer-like cell line (YT cells). *J. Immunol.*, **134**, 1623–1630.

Zachowski,A. (1993) Phospholipids in animal eukaryotic membranes: transverse assymmetry and movement. *Biochem. J.*, **294**, 1–14.

*Received on July 28, 1997; revised on October 3, 1997*